**The cholesterol biosynthesis pathway regulates IL-10 expression in human Th1 cells.**

**Perucha E et al.**

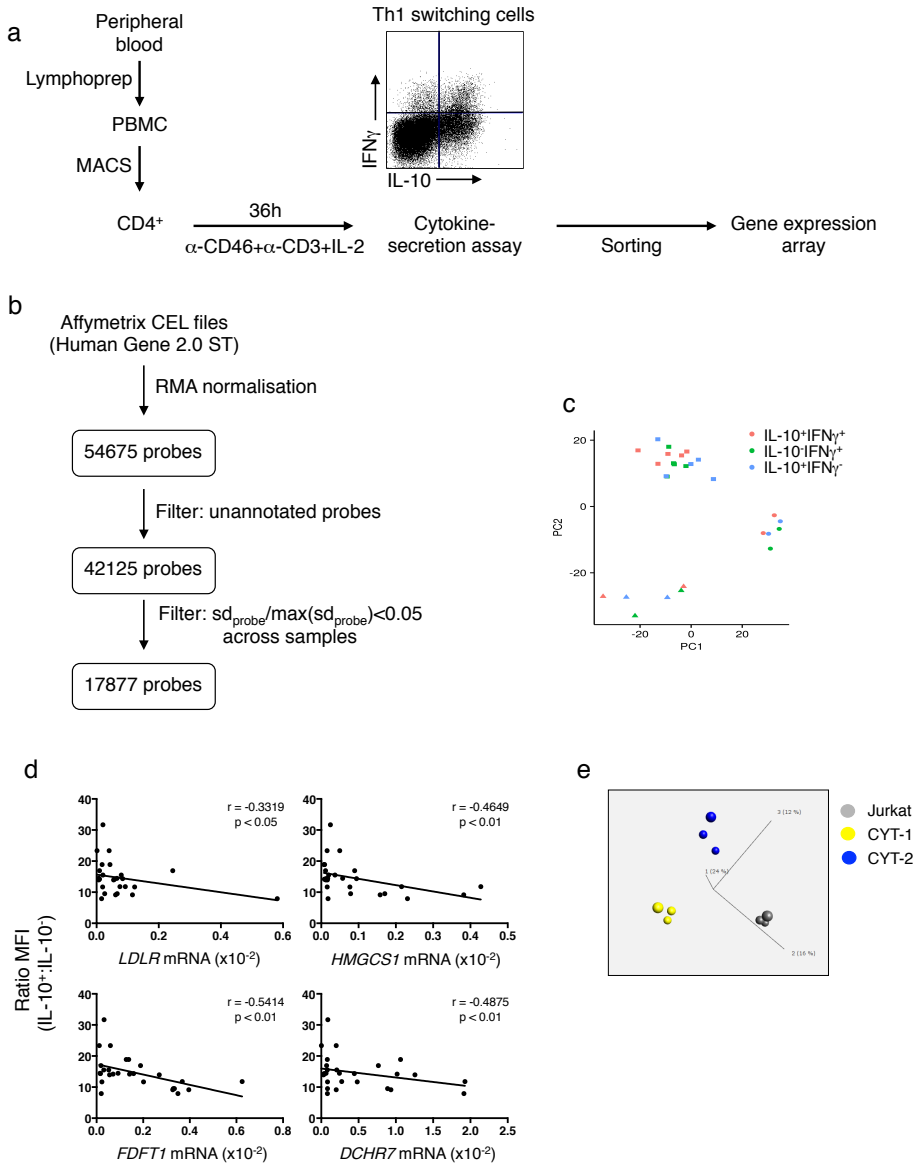


**Supplementary Figure 1. Metabolic regulation of Th1 switching in primary human CD4$^+$ T cells.** (**a**) Schematic representation of the experimental set-up leading to Th1 switching cells and gene expression array experiments. (**b**) Schematic representation of the micro-array analysis workflow. (**c**) Clustering analysis of gene expression data on IFNγ$^+$IL-10$^-$ (green), IFNγ$^+$IL-10$^+$ (red) and IFNγ$^-$IL-10$^+$ (blue) populations. (**d**) Relation between mRNA levels of cholesterol biosynthesis pathway selected targets in the IFNγ$^-$IL-10$^-$ and IFNγ$^+$IL-10$^-$ populations and the MFI ratio for IL-10 (IFNγ$^+$IL-10$^+$:IFNγ$^-$IL-10$^-$) (n=14), showing a linear regression for each gene. R and p values for one-tailed Spearman test for each target are shown. (**e**) Principal component analysis of gene expression array derived from control Jurkat T cells *versus* Jurkat-CYT-1 *versus* Jurkat-CYT-2 expressing cells.

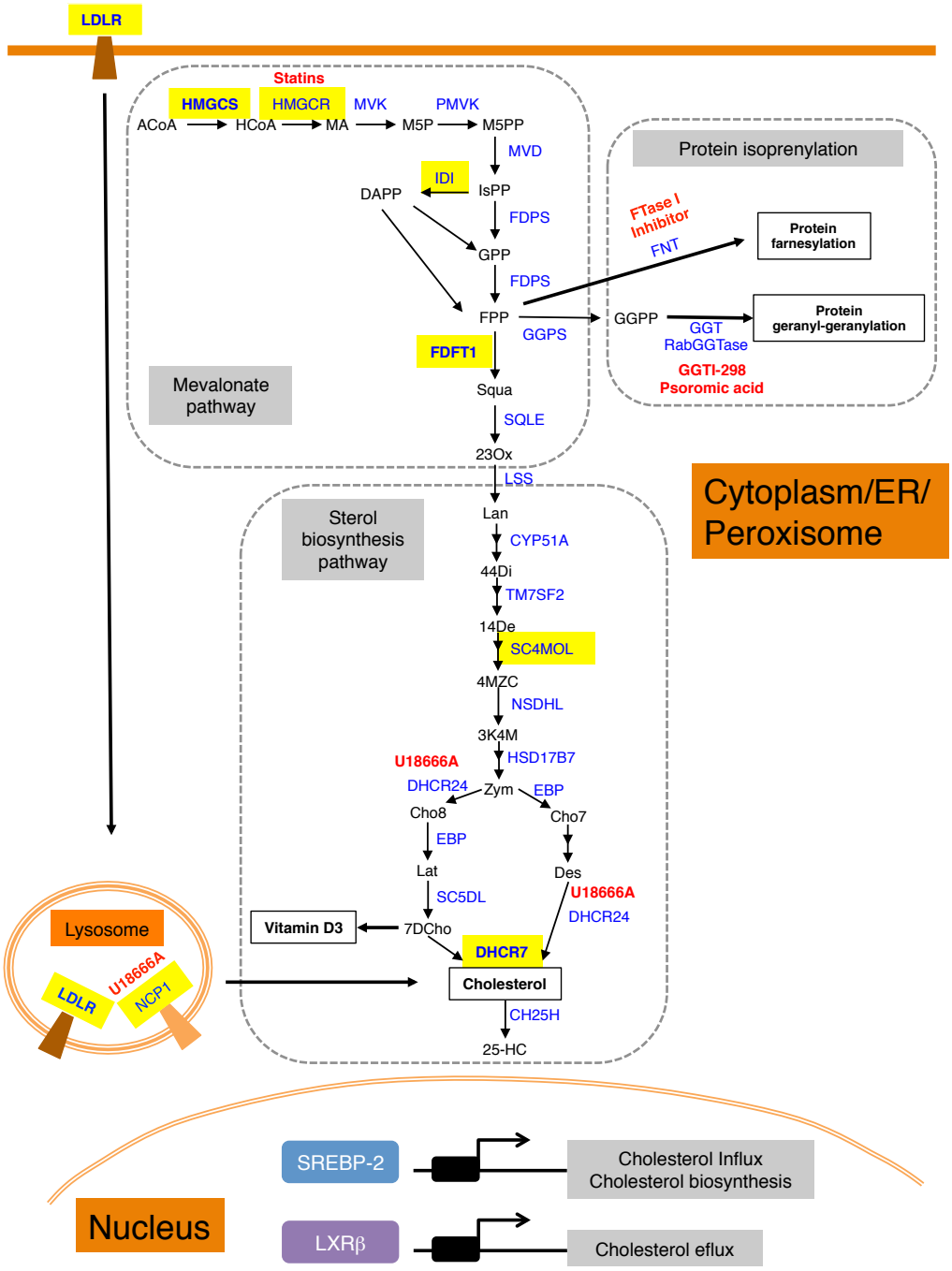


**Supplementary Figure 2. Schematic representation of the cholesterol biosynthesis pathway and its regulation.** Metabolites of the pathway are shown in black, enzymes of the pathway are shown in blue and inhibitors are shown in red. The pathway is regulated by two master transcription factors: Liver X receptor β (LXRβ) negatively regulates the pathway by promoting cholesterol efflux while Sterol Regulatory Element-Binding Protein-2 (SREPB-2) positively regulates the pathway by promoting the transcription of the enzymes implicated in the pathway as well as cholesterol import via the LDLr. Probes significantly associated with IL-10 levels (Fig. 1b) are highlighted in yellow. Legend with full names is provided in Supplementary Table 1.

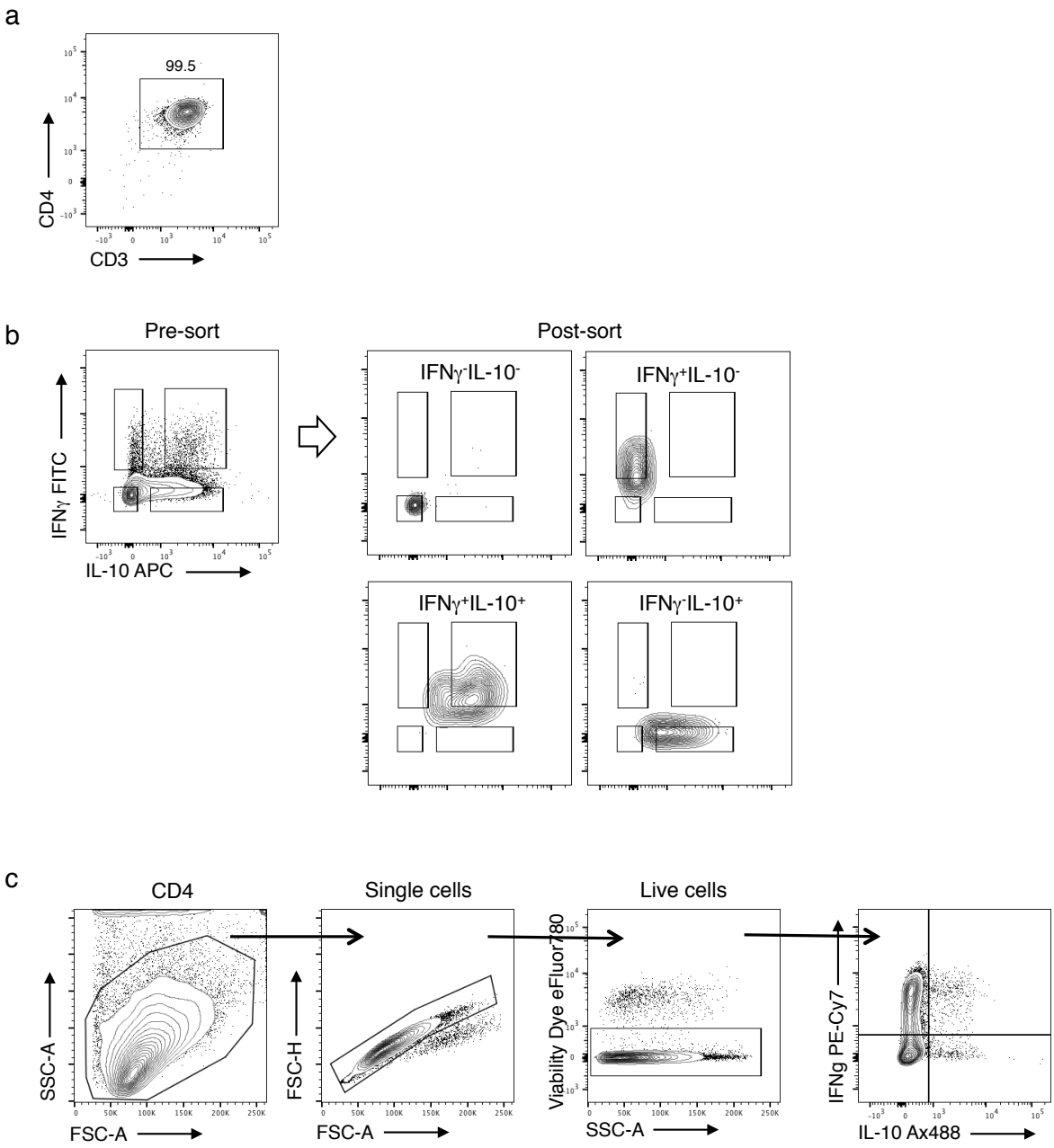


**Supplementary Figure 3. Gating strategies.** Purified human $CD4^+$ T cells stimulated *in vitro* with plate bound $\alpha$-CD3 (2 $\mu$g $ml^{-1}$) + $\alpha$-CD46 (5 $\mu$g $ml^{-1}$) + rhIL-2 (50 U $ml^{-1}$) were cultured for 36 hours. (**a**) Representative $CD4^+$ purity gating. (**b**) Gating strategy and post-sort analysis for cytokine secretion assay presented in Fig. 1 and Supplementary Fig. 1. (**c**) Gating strategy for intracellular cytokine staining analysis presented in Fig. 2, 3, 4 and Supplementary Fig. 4, 6.

.

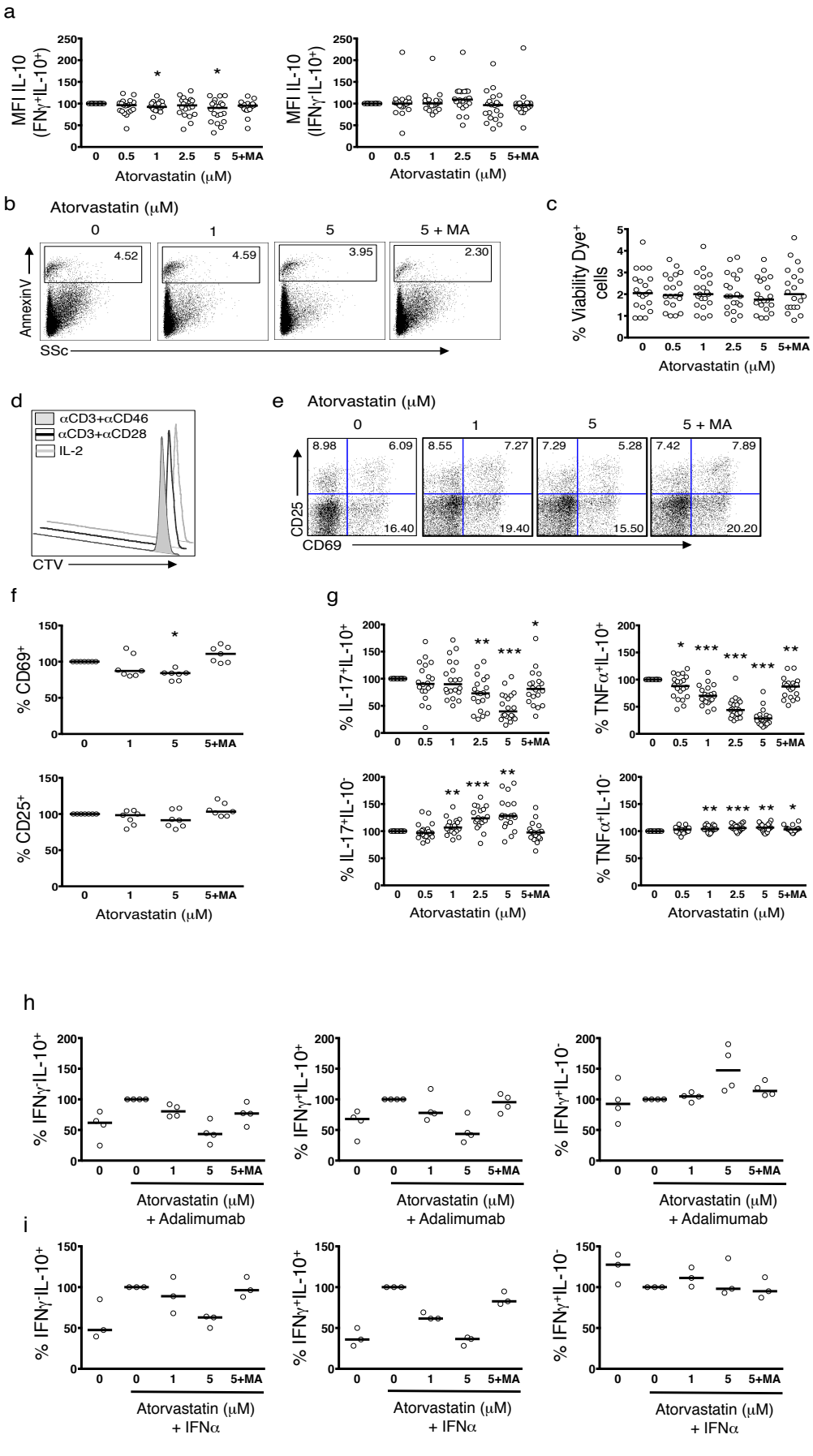
a
MFI IL-10 (FNγ+IL-10+)
MFI IL-10 (IFNγ-IL-10+)
Atorvastatin (μM)
b
Atorvastatin (μM)
0
1
5
5 + MA
4.52
4.59
3.95
2.30
AnnexinV
SSc
c
% Viability Dye+ cells
Atorvastatin (μM)
d
αCD3+αCD46
αCD3+αCD28
IL-2
CTV
e
Atorvastatin (μM)
0
1
5
5 + MA
8.98
6.09
16.40
8.55
7.27
19.40
7.29
5.28
15.50
7.42
7.89
20.20
CD25
CD69
f
% CD69+
% CD25+
Atorvastatin (μM)
g
% IL-17+IL-10+
% TNFα+IL-10+
% IL-17+IL-10-
% TNFα+IL-10-
Atorvastatin (μM)
h
% IFNγ-IL-10+
% IFNγ+IL-10+
% IFNγ+IL-10-
Atorvastatin (μM)
+ Adalimumab
i
% IFNγ-IL-10+
% IFNγ+IL-10+
% IFNγ+IL-10-
Atorvastatin (μM)
+ IFNα

**Supplementary Figure 4. Th1 switching to IL-10 is blocked when the mevalonate pathway is inhibited.** Purified human $CD4^+$ T cells stimulated *in vitro* with plate bound α-CD3 (2 μg $ml^{-1}$) + α-CD46 (5 μg $ml^{-1}$) + rhIL-2 (50 U $ml^{-1}$) were cultured for 36 hours in the presence of atorvastatin and 250 μM mevalonic acid (MA) as indicated, unless stated otherwise. (**a**) Normalised mean fluorescence intensity (MFI) for IL-10 in $IFN\gamma^+IL\text{-}10^+$ (left) and $IFN\gamma^-L\text{-}10^+$ (right) cells (n=20). (**b**) Representative dot-plots for annexin staining on treated cells (data are representative of 5 independent donors). (**c**) Percentage of fixable viability dye positive cells (n=20). (**d**) Representative histogram of Cell Trace Violet (CTV) staining of $CD4^+$ T cells stimulated in vitro with IL-2, α-CD3 + α-CD46 or beads coated with α-CD3 + α-CD28 for 36 hours (data are representative of 3 independent donors). (**e**) Representative dot-plot of $CD69^+$ and $CD25^+$ surface staining. (**f**) Normalised frequency of $CD69^+$ (left) and $CD25^+$ (right) cells (n=7). (**g**) Normalised frequency of $IL\text{-}17^+IL\text{-}10^+$ (top left), $IL\text{-}17^+IL\text{-}10^-$ (bottom left), $TNF\alpha^+IL\text{-}10^+$ (right left), $TNF\alpha^+IL\text{-}10^-$ (bottom right) producing cells (n=20). (**h**) Normalised frequency of $IL\text{-}10^+IFN\gamma^-$ (left), $IFN\gamma^+L\text{-}10^+$ (centre) and $IFN\gamma^+IL\text{-}10^-$ (right) $CD4^+$ T cells co-cultured with monocytes and α-CD3 (100 ng $ml^{-1}$) in the absence or presence of Adalimumab (1 μg $ml^{-1}$) and treated with atorvastatin and MA (n=4). (**i**) Normalised frequency of $IL\text{-}10^+IFN\gamma^-$ (left), $IFN\gamma^+L\text{-}10^+$ (centre) and $IFN\gamma^+IL\text{-}10^-$ (right) $CD4^+$ T cells activated for 3 days with plate bound α-CD3 (0.5 μg $ml^{-1}$) + α-CD28 (1 μg $ml^{-1}$) + IFNα (600 U $ml^{-1}$) and treated with atorvastatin and MA (n=3). Graphs show independent donors (dots) normalised to 0 dose of atorvastatin; bars represent median values. *<0.05, **<0.01 and ***<0.001 denote a significant difference compared to untreated cells by repeated measures one-way ANOVA test with *post hoc* Dunnett's correction (a, c, g) or Friedman test with *post hoc* Dunn's correction (f).

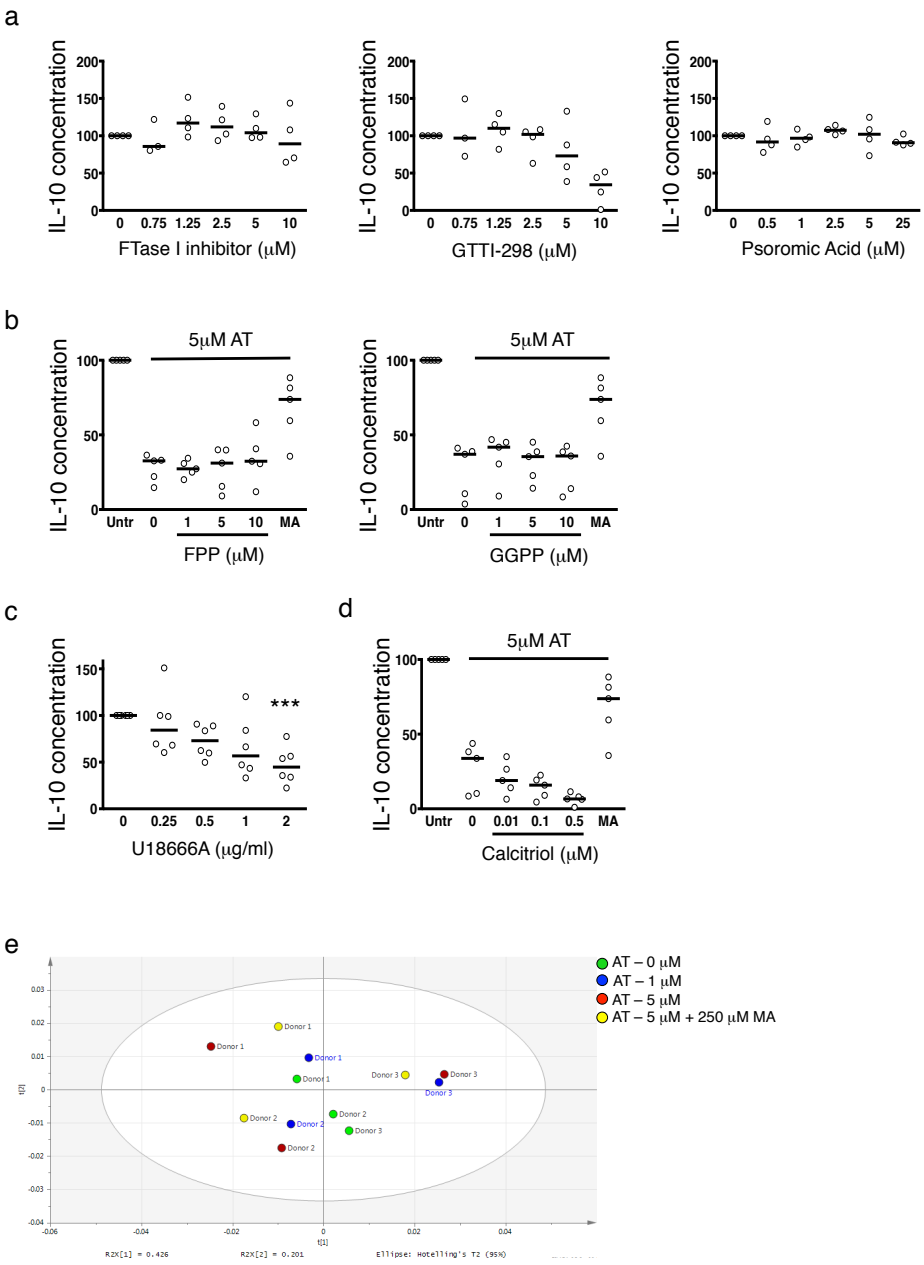


**Supplementary Figure 5. IL-10 regulation in Th1 switching cells is dependent on fit CBP metabolism, but not on isoprenylation, vitamin D3 or cellular cholesterol content.** Purified human $CD4^+$ T cells stimulated *in vitro* with plate bound α-CD3 (2 μg $ml^{-1}$) + α-CD46 (5 μg $ml^{-1}$) + rhIL-2 (50 U $ml^{-1}$) were cultured for 36 hours in the presence of selected metabolites and inhibitors as indicated. (**a**) Normalised concentrations of secreted IL-10 by cells cultured in the presence of inhibitors for farnesyl-PP transferase (FTase I inhibitor) (left), geranylgenaryl-PP synthase (GGTI-298) (centre) and Rab geranylgeranyltransferase (psoromic acid) (right) (n=4). (**b**) Normalised concentrations of secreted IL-10 by cells cultured with 5 μM atorvastatin (AT) and increasing concentrations of farnesylpyrophosphate (FPP) (left) and geranylgeranylphyrophosphate (GGPP) (right) and mevalonic acid (MA) as control (n=5). (**c**) Normalised concentrations of secreted IL-10 by cells cultured in the

presence of increasing concentrations of U1866A (n=6). (**d**) Normalised concentrations of secreted IL-10 by cells cultured with 5 μM atorvastatin (AT) and increasing concentrations of calcitriol and mevalonic acid (MA) as control (n=5). (**e**) Principal component analysis of lipidomics analysis of cells treated with atorvastatin (AT) and mevalonic acid (MA) (n=3). Graphs show independent donors (dots) normalised to untreated cells; bars represent median values. *P* values: ***<0.001 denote a significant difference compared to untreated cells by Friedman test with *post hoc* Dunn's correction for multiple comparisons.

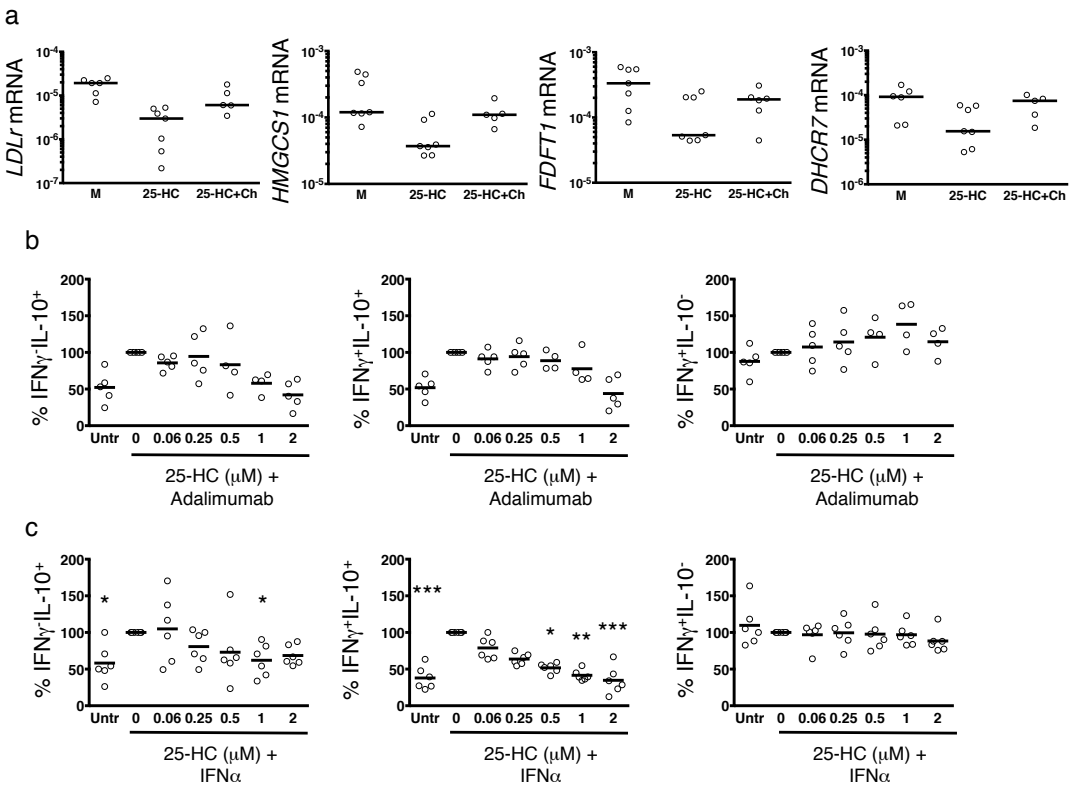


**Supplementary Figure 6. IL-10 expression in Th1 switching cells is dependent on intact cholesterol pathway fitness.** Purified human $CD4^+$ T cells stimulated *in vitro* with plate bound $\alpha$-CD3 (2 $\mu$g $ml^{-1}$) + $\alpha$-CD46 (5 $\mu$g $ml^{-1}$) + rhIL-2 (50 U $ml^{-1}$) were cultured for 36 hours in the presence of 25-hydroxycholesterol (25-HC) and different media conditions as indicated. (**a**) Normalised *LDLr*, *HMGCS1*, *FDFT1* and *DHCR7* mRNA levels of cells cultured in fully supplemented media (M), 25-HC (2 $\mu$M) with or without cholesterol 500x (Ch) (n=5-7). (**b**) Normalised frequency of $IL\text{-}10^+IFN\gamma^-$ (left), $IFN\gamma^+L\text{-}10^+$ (centre) and $IFN\gamma^+IL\text{-}10^-$ (right) $CD4^+$ T cells co-cultured with monocytes and $\alpha$-CD3 (100 ng $ml^{-1}$) in the absence or presence of Adalimumab (1 $\mu$g $ml^{-1}$) and treated with 25-HC (n=5). (**c**) Normalised frequency of $IL\text{-}10^+IFN\gamma^-$ (left), $IFN\gamma^+L\text{-}10^+$ (centre) and $IFN\gamma^+IL\text{-}10^-$ (right) $CD4^+$ T cells activated for 3 days with plate bound $\alpha$-CD3 (0.5 $\mu$g $ml^{-1}$) + $\alpha$-CD28 (1 $\mu$g $ml^{-1}$) + IFN$\alpha$ (600 U $ml^{-1}$) and treated with 25-HC (n=6).

**Supplementary table 1: Supplementary Figure 2 legend.**

**Metabolites**

| | |
|---|---|
| ACoA | Acetyl-CoA |
| HCoA | 3-hydroxy-3-methylglutaryl-CoA |
| MA | Mevalonic Acid |
| M5P | Mevalonate-5-phosphate |
| M5PP | Mevalonate-5-pyrophosphate |
| IsPP | Isopentenyl-5-pyrophosphate |
| DAPP | Dimethylallyl-PP |
| GPP | Geranyl-PP |
| FPP | Farnesyl-PP |
| GGPP | Geranylgeranyl-PP |
| Squa | Squalene |
| 23Ox | 2,3-oxidosqualene |
| Lan | Lanosterol |
| 44Di | 4,4'-dimethyl-cholesta-8,14,24-trieneol |
| 14De | 14-demethyl-lanosterol |
| 4MZC | 4-methylzymosterol-carboxylate |
| 3K4M | 3-keto-4-methyl-zymosterol |
| Zym | Zymosterol |
| Cho7 | Cholesta-7,24-dien-3beta-ol |
| Des | Desmosterol |
| Cho8 | Cholesta-8,en-3beta-ol |
| Lat | Lathosterol |
| 7DCho | 7-dehydrocholesterol |
| 25HC | 25-hydroxycholesterol |

**Enzymes/proteins**

| | |
|---|---|
| HMGCS | 3-hydroxy-3-methylglutaryl-CoA synthase |
| HMGCR | 3-hydroxy-3-methylglutaryl-CoA reductase |
| MVK | Mevalonate Kinase |
| PMVK | Phosphomevalonate kinase |
| MVD | Mevalonate-5-pyrophosphate decarboxilase |
| FDPS | Farnesyl-PP synthase |
| IDI | Isopentenyl-PP isomerase |
| FNT | Farnesyltransferase |
| GGPS | Geranylgeranyl-PP synthase |
| GGT | Geranylgeranyl transferase |
| RabGGTase | Rab geranylgeranyl transferase |
| FDFT1 | Farnesyl-PP farnesyltransferase 1 (squalene synthase) |
| SQLE | Squalene epoxydase |
| LSS | Lanosterol synthase |
| CYP51A | Lanosterol 14 alpha-demethylase |
| TM7SF2 | Delta(14)-sterol reductase |
| SC4MOL (MSMO1) | Methylsterol Monooxygenase 1 |

| | |
|---|---|
| NSDHL | Sterol-4-alpha-carboxylate 3-dehydrogenase |
| HSD17B7 | 3-ketosteroid reductase |
| DHCR24 | 24-dehydrocholesterol reductase |
| EBP | Sterol isomerase |
| SCD5L | Lathosterol oxidase |
| DHCR7 | 7-dehydrocholesterol reductase |
| CH25H | 25-hydroxycholesterol hydroxylase |
| NPC1 | Niemann-Pick disease, type C1 |
| LDLR | Low density lipoprotein receptor |